Available online at www.sciencedirect.com
SCIENCE DIRECT®
Journal of Nuclear Materials 328 (2004) 107–114
journal of nuclear materials
www.elsevier.com/locate/jnucmat

Vacancy cluster evolution and swelling in irradiated 316 stainless steel

Michael P. Surh, J.B. Sturgeon *, W.G. Wolfer

Lawrence Livermore National Laboratory Livermore, L-353, P.O. Box 808, Livermore, CA 94550, USA

Received 25 November 2003; accepted 2 March 2004

Abstract

A recently developed master equation and Fokker–Planck method for cluster-nucleation and growth simulations is applied to a model of impurity-free type-316 stainless steel under irradiation. The evolution of the void size distribution is treated in full generality, although the dislocation density is held constant versus time and temperature. The simulations reproduce several observed characteristics of irradiation swelling, involving a brief incubation delay followed by quasi-steady swelling. The predicted incubation period shows a clear dose-rate response – lower irradiation flux requires less total fluence to complete the incubation process. This trend is consistent with some recent experimental reports.

1. Introduction

With more than three decades worth of data from irradiated austenitic stainless steels, it has become clear that void swelling eventually (after accumulating sufficient displacement damage) develops over a wide range of irradiation temperatures. Temperatures that promote void swelling range from the onset of vacancy migration in the material (about 300 °C for austenitic steels) to regions where self-diffusion dominates (about 650 °C). Under these conditions, void swelling advances gradually with increasing time or displacement dose, commencing at a negligible rate, accelerating with dose by some power greater than one, and inexorably proceeding to a steady-state increase nearly linear with dose. The gradual or non-linear onset of swelling delimits an initial, 'transient' period. Extrapolation of the subsequent, linear, steady-state behavior to lower doses gives an intercept at zero swelling, which may be taken to define an 'incubation' dose for void swelling. Alternatively, experimental analyses sometimes use another empirical definition equal to the cumulative dose to reach volumetric swelling of 1%. For clarity, neither definition of incubation is identical to the transient period, although they are obviously all related.

It is worth noting that both (macroscopic) void swelling and (microscopic) void nucleation possesses initial, incubation delays. The two intervals are not the same. Originally, 'incubation' is used in classical nucleation theory to specify the delay to steady nucleation of stable clusters. Specifically, it refers to the comparatively short period before the rate of void nucleation reaches the quasi-stationary value predicted by classical nucleation theory. However, in the radiation damage literature, it now customarily refers to the delay to steady swelling. In the discussion presented here, 'incubation' will refer to macroscopic swelling, in order to make connection with experimental observations.

Incubation doses for austenitic stainless steels range from a few tenths to tens of displacements per atom (dpa). Subsequently, the volume increases at 1%/dpa, which rapidly alters the engineering properties of the material. Thus, the incubation behavior defines to a large extent the useful lifetime of a component in a reactor. Metallurgists seek to prolong this period by

* Corresponding author.
E-mail address: sturgeon2@llnl.gov (J.B. Sturgeon).

0022-3115/$ - see front matter
doi:10.1016/j.jnucmat.2004.03.005

changing the composition and metallurgical processing of the steel, or by developing new materials not in the family of austenitic steels.

The various stages of swelling are believed to develop similarly in many different materials. An example is shown in Fig. 1, for solution-annealed 304 stainless steel irradiated in EBR II. Macroscopic measurements do not readily differentiate these various regimes of behavior. Therefore, lengthy exposures may be required to complete the incubation process and fully isolate the asymptotic behavior. It now seems that the true steady-state swelling is largely independent of initial impurities, initial dislocation density, system temperature, and irradiation dose-rate [1–9]. Only the duration of the incubation period appears to depend on these parameters. Early analyses generally assume that the incubation period would be independent of dose-rate. As a result, experiments with limited exposures may confuse steady-state behavior with the late stages of the transient period. In such cases, a spurious temperature or dose-rate dependence may be imputed to the steady-state.

Most importantly, this new interpretation discerns an incubation 'dose-rate effect', i.e., that a lower irradiation dose-rate requires a smaller cumulative fluence to complete the incubation process [4–9] (see also Fig. 1). This

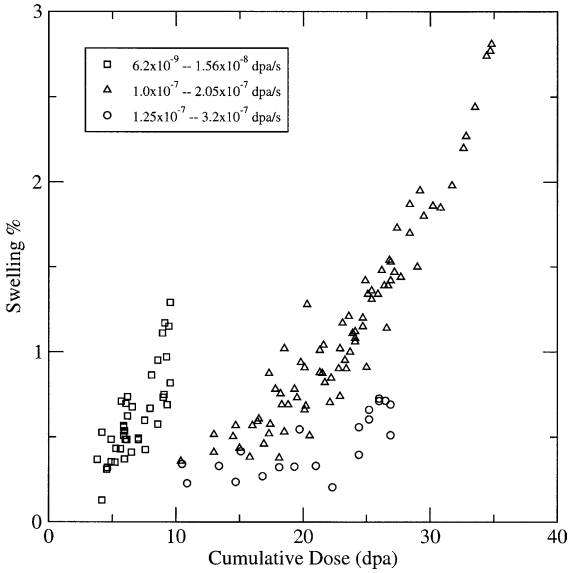

Fig. 1. Void swelling in solution-annealed 304 stainless steel irradiated in the reflector and blanket regions of EBR-II. Data are grouped according to the dose-rates indicated in the insert. The onset of irradiation triggers the formation of small defect clusters but causes very little volumetric expansion. This is followed by an incubation period consisting of void accumulation and growth and accelerating void swelling. This eventually reaches a steady-state swelling rate around 1%/dpa for austenitic steel (as indicated by the solid line).

relation will impact next-generation reactor designs that operate at historically low dose-rates or higher temperatures than current facilities. Reactor components subjected to these conditions may swell sooner than previously anticipated. Such a possibility calls for new experimental and theoretical efforts to better understand the transient behavior of irradiation-induced swelling.

Prior theory and modeling of radiation-induced void swelling falls into two categories. The first models emphasize the growth of voids once nucleated. They assume that voids begin to nucleate early on, and that the deterministic growth of these cavities dictates swelling behavior. Void nucleation is included at a steady-state rate, but without a self-consistent provision to terminate the nucleation process and limit the final density of voids. This steady-state theory does not provide the final number density of voids that can be compared with experimental results [10]. A second category of theory seeks more detailed descriptions of time-dependent void nucleation. Such schemes have long been available, but their use in the analysis of actual data has been limited [11]. Time-dependent calculations have previously been too slow to reach doses required to complete incubation (tens of dpa, in materials like austenitic steels) [12].

Now, a new master equation/Monte Carlo hybrid method enables the renewed pursuit of a time-dependent void nucleation and growth theory, with the goal to eventually predict void swelling in all of its stages. Our numerical implementation of the rate theory method [12,13] has been described in Refs. [14,15]. This method will allow us to systematically incorporate the various processes believed to influence void swelling, such as defect trapping by impurities, concurrent loop and network dislocation evolution, radiation-induced segregation and its effect on bias factors, 'production bias' and low-dimensional cluster diffusion, etc.

This paper is the first in a series that will examine the nucleation and growth of voids and the time-dependent swelling of irradiated metals. We extend earlier simulations of void nucleation and growth to higher radiation fluences and swelling, and study the systematic dependence on environmental parameters. The void size distribution is modeled in full generality, from monomers to clusters of arbitrary size, but with time-independent network dislocation density (as in Ref. [12]). Network dislocation bias factors are calculated for a fixed dislocation density of 6×10^{14} m^{-2}, irrespective of the density used to calculate dislocation sink strengths. Dislocation loops are not included separately from the network dislocation content. This is the same model used in Ref. [12], chosen here for continuity with that earlier work. The constant dislocation density model also serves to isolate the effect of void nucleation and growth on the swelling, separately from other, concurrent changes in the microstructure. It is in this reductionist approach

that the simulations have their greatest value. This simplified model demonstrates that the details of void nucleation can reproduce many features seen experimentally. Comparing these results to a model with co-evolving dislocation content will show how the self-consistent interplay of irradiation damage with voids and dislocations acts to shape the steady swelling behavior. This comparison is deferred to a companion paper, next in the planned series of studies.

Here, we compare our results from the constant dislocation density model with two experimental observations, macroscopic volumetric swelling being the first and most prominent. Irradiation-induced changes to other macroscopic properties like ductility and hardness are dependent on defect–defect interactions, and are not directly obtained from our simulations. More detailed, microscopic measurements of void densities versus size are also available from TEM experiment. However, small sample sizes and the limits of instrumental resolution complicate the experimental analysis of void populations [16]. Accordingly, we limit our second comparison to the total density of voids above 0.5 nm radius (the 'visible' void number density). Neglecting void volume relaxation, these two quantities relate to the first and zeroth moments, respectively, of the void size distribution, $\rho(n)$, with respect to the size of the void in terms of the number, n, of vacancies.

Already, our simplified microstructure model predicts some trends that are in general agreement with experiment. The simulated incubation exhibits a dose-rate effect wherein lower fluxes require smaller incubation doses, consistent with the behavior of commercial alloys. The result is obtained even though the model is confined to void evolution alone, lending support to our void nucleation-and-growth approach to studying initial swelling behavior. It is notable that our predicted incubation times are on the order of 1–10 dpa, much shorter than are seen in commercial austenitic alloys. These values are approximately consistent with recent experiments in pure ternary stainless steels, suggesting an important role for impurities and precipitates in prolonging incubation. However, a flux-independent incubation time has been reported for high-purity steels. The simulated effect is less extreme in its magnitude.

2. Results

Void evolution simulations are performed for precipitate-free, solute-free, type-316 austenitic stainless steel. The model material parameters in Table 1 are taken from separate studies of dislocation and void evolution under irradiation [12,13]. Multiple calculations span three different irradiation dose rates (10^{-6}, 10^{-7} and 10^{-8} dpa/s) and temperatures from 280 to 700 °C. The dislocation density is held constant at values ranging from 2×10^{13} to 6×10^{15} m^{-2}. Time-steps are set so as to maintain conservation of mass at parts in 10^3 to 10^5 of the net swelling. The time evolution begins with intervals of 10^{-5} s, which increase exponentially to follow the transient formation of vacancy dimers, trimers, etc. Time-steps reach a maximum of 500, 2000, or 32 000 s for fluxes of 10^{-6}, 10^{-7} and 10^{-8} dpa/s, respectively, regardless of temperature or dislocation density.

Table 1
Model materials parameters for type-316 stainless steel

Cascade efficiency	0.1
Lattice parameter, a_0	0.3639 nm
Burgers vector	0.2573 nm
Shear modulus	82.95 GPa
Poisson's ratio	0.264
Vacancy migration energy	1.92×10^{-19} J
Vacancy formation energy	2.88×10^{-19} J
Pre-exponential factor, D_v^0	1.29×10^{-6} m^2/s
Vacancy relaxation volume	$-0.2\ \Omega$
Interstitial relaxation volume	$1.5\ \Omega$
Vacancy shear polarizability	-2.4×10^{-18} J
Interstitial shear polarizability	-2.535×10^{-18} J
Vacancy-interstitial recombination radius	0.7278 nm
Void surface energy	$3.01–0.55\times10^{-3}$ T (J/m^2)

The initial volume changes predicted by our model are shown in Fig. 2 for several temperatures. (The fixed dislocation density of 6×10^{14} m^{-2} is chosen because it roughly corresponds to the asymptotic values seen in heavily irradiated stainless steels across a wide range of temperatures. Thus, the simulation approximates a hypothetical situation in which the material is cold-worked to the expected ultimate dislocation density

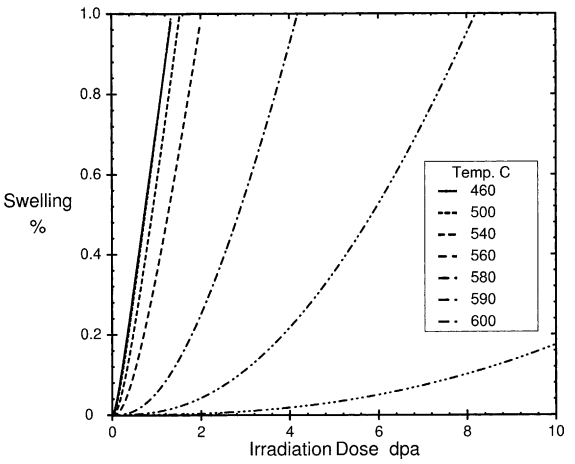

Fig. 2. Fractional volumetric swelling, $\Delta V/V$, from void nucleation and growth simulations at a constant dislocation density of 6×10^{14} m^{-2} and 10^{-6} dpa/s irradiation.

before beginning the experiment. In this case, the dislocation content might be expected to remain roughly constant during irradiation.) The simulated void swelling reveals two qualitatively different regimes of behavior. In the first, the swelling rate is small but supra-linear in time. This initial behavior persists until the simulation either ends (at 100 dpa) or the swelling rate reaches a maximum instantaneous value (at most around 1%/dpa). A second regime of behavior subsequently shows quasi-steady swelling, although the swelling rate decreases towards much later times (see also Fig. 3). The behavior can be understood in terms of the relative sink strengths of voids and dislocations [17].

The predicted volumetric swelling versus irradiation dose is shown again in Fig. 4 for the same temperature range and dose-rate as above, but for longer times. The sequence of temperatures can be difficult to follow due to crossing of the curves, so fewer cases are shown here. The higher temperature simulations have longer delays to the onset of quasi-steady swelling, but they also eventually reach higher swelling rates.

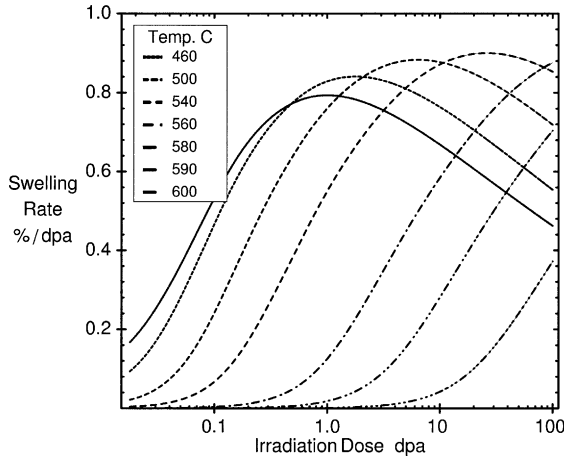

Fig. 3. Volumetric swelling rate, $\frac{d\Delta V/V}{dt}$, versus dose from the data in Fig. 1 shown over longer times.

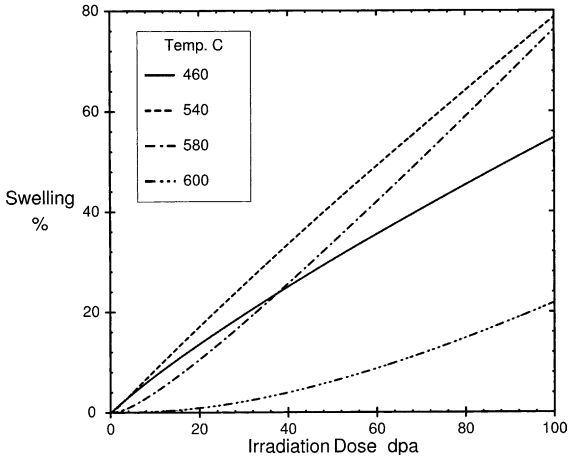

Fig. 4. Volumetric swelling curves at a dose-rate of 10^{-6} dpa/s and dislocation density of 6×10^{14} m^{-2} for the duration of the simulations.

The simulations reproduce three important characteristics seen in experiment. At the outset, there is often a transient delay to the simulated response, which can be identified with the experimental incubation behavior. Subsequently, the quasi-steady swelling rate is quantitatively comparable to the experimental value. Finally, the predicted duration of the incubation delay versus temperature and dose-rate confirm the experimental dose-rate effect seen in commercial alloys.

The experimental incubation behavior includes small amounts of initial swelling which increase in rate versus time until the steady-state is reached. Thus, the simulated transient behavior is at least qualitatively consistent with observations. The swelling delay arises because a population of stable voids is required to enable the preferential segregation of interstitials to dislocations and vacancies to cavities. Stable voids simply have not nucleated to a sufficient density or reached appreciable aggregate sink strengths at early times.

The subsequent peak and quasi-steady swelling rates are most easily seen in Fig. 3. These typically lie between 0.7 and 1.0%/dpa, consistent with the experimental rate for stainless steels around 1%/dpa [1]. However, the predicted swelling rates drop off with time, falling as low as 0.4%/dpa. This behavior is not commonly seen in commercial, or high-purity steels [4]. It is also evident that the predicted steady swelling rate is temperature-dependent in this temperature range, contrary to experiment [1–4]. True saturation (i.e. cessation of swelling [1]) never occurs in these simulations, although the swelling rate is expected to continue to decline as the void sink strengths grow without bounds. (In fact, the model is not strictly applicable at doses of 100 dpa, because the mean-field assumption of small, well-separated voids is obviously no longer valid when the overall volume has doubled. At the least, the possibilities of dislocation–void and void–void impingement and coalescence have not been included.)

Despite the qualitative similarity between predicted and observed transient behavior, the simulated swelling delay is not in quantitative agreement with most experiments. The observed incubation times in commercial steels can be very long, even exceeding 100 dpa. In contrast, the simulated incubation is not even visible in the swelling curves at some temperatures, dose-rates, and dislocation densities in our model of pure, precipitate-free steel. However, the predicted brevity is closer to recent measurements in high purity stainless steels [6–9]. Thus, the difference likely reflects the importance of impurities and precipitates in delaying the onset of steady swelling.

At the upper temperature limit studied, the total swelling remains negligible during the finite simulation interval because the void nucleation time diverges with temperature. In such extreme cases, swelling approaches a power-law dependence versus time, and the change from incubation to steady-behavior is most gradual when the simulated incubation is longest. This behavior is qualitatively different from experimental observations. The experimental swelling seems to switch from incubation to steady-behavior more abruptly after longer incubation delays [4]. This discrepancy is also likely due to the influence of other, co-evolving components of the microstructure (such as the dislocation or precipitate distributions) that are held constant or are absent in the simple model employed here.

The calculated swelling curves may be used to quantify an incubation time by following the same procedures as are used in analyzing experimental swelling curves. For example, incubation is sometimes defined experimentally as the cumulative dose to reach (the arbitrarily chosen value of) 1% swelling. The dependence of this measure on temperature and dose-rate is shown in Figs. 5 and 6, for different dislocation densities. The lower value of 2×10^{13} m^{-2} shown in Fig. 5 is representative of the starting state for a solution annealed stainless steel. The higher value of 6×10^{14} m^{-2} in Fig. 5 approximates the asymptotic density for irradiated steels over a wide range of temperatures.

At increasing temperature, the critical size for stable voids, n_{crit}, diverges, so that it becomes difficult to nucleate stable voids. (Void stability is defined from the size-dependent Fokker-Planck drift parameter, $K(n) > 0$.) As a consequence of the slow nucleation rate, the incubation doses in Figs. 5 and 6 increase steeply with temperature at the upper limits shown. In this region, higher dose-rates mainly shift the onset of swelling to higher temperatures.

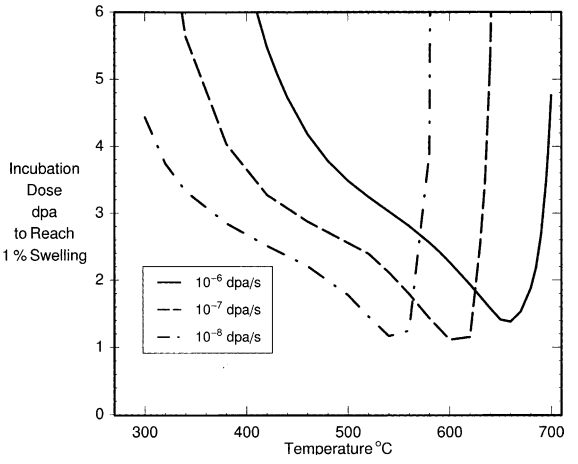

Fig. 5. Predicted incubation dose for 316 stainless steel with a constant dislocation density of 2×10^{13} m^{-2}, and three different dose-rates.

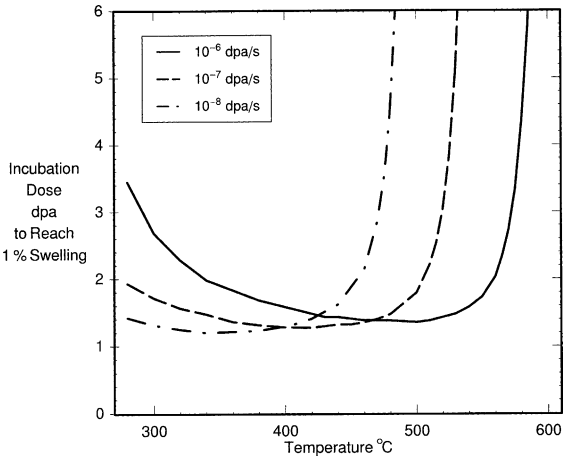

Fig. 6. Incubation dose for 316 stainless steel with a constant dislocation density of 6×10^{14} m^{-2}, and three different dose-rates.

To a first approximation, the incubation curves at three different dose rates have the same shapes. Each simulated curve possesses a minimum incubation dose versus temperature, which is shifted to higher temperatures for the higher dose-rates [18]. The predicted incubation doses never fall below 1 dpa. This is because the peak rate of swelling is always less than 1%/dpa (excluding the transient formation of dimers and other small, unstable clusters that occupies the first minutes of the simulation). Thus, there must be at least 1 dpa of irradiation to reach $\Delta V/V = 1\%$.

Figs. 5 and 6 both show that the displacement of the lower dose-rate curves gives smaller incubation doses up to temperatures of 400–500 °C. This is a preliminary confirmation of the experimental dose-rate effect seen in commercial alloys [4]. However, this offset behavior is not consistent with what is seen in high purity alloys, where the measured incubation dose is inversely related to flux [6]. In this case, there is a universal incubation time, independent of the dose-rate. Rigidly shifting the incubation curves for different fluxes can give this relation only by accident. It is possible that the total incubation delay is so short here that it is dominated by an initial, flux-independent stage, while the simulations only model a second, flux-dependent part to the incubation interval. Finally, this comparison is complicated by the fact that incubation is defined differently here than it is in these experiments. The experimental measure extrapolates from the steady-state swelling curve back to zero swelling. Using that definition to analyze the simulations does change the predicted shapes of the incubation curves, but it does not seem to lead to an inverse dose-rate effect.

Besides macroscopic volumetric changes, the numerical simulations provide a wealth of information on the distribution of void sizes. Comparable TEM observations are subject to statistical and measurement uncertainties. Thus, we only examine the predicted total density of voids with radii greater than 0.5 nm, a rough limit of resolution for TEM. The overall behavior may be seen in Fig. 7, which shows the visible void density versus time for a range of temperatures. A second limit in TEM observation is set by the small sample volumes; as a result, void densities below 5×10^{18} m^{-3} are also effectively undetectable. This second limit is denoted with a horizontal, dashed line – for completeness, the time-evolution is also shown for undetectably small densities. At moderate temperatures, the visible void density quickly reaches a saturation value essentially equal to the density of stable voids. These stable voids continue to grow in size for the duration of the simulation, while no further stable voids appear. However, this short nucleation time is not seen experimentally; void densities are seen to increase in high purity steels after sequential irradiation exposures even after tens of dpa [19].

In practice, the simulated asymptotic or terminal void number density is reached (in solution annealed material at moderate temperature) before the initial dislocation content has time to change appreciably. Thus, the predicted, terminal void density is controlled by the initial dislocation density (besides the temperature and dose-rate). While the asymptotic dislocation density should influence the swelling rate at later times, it does not affect the number of voids. Therefore, when comparing the calculated void content to experiment on solution annealed samples, our constant dislocation density model should be fit to the initial dislocation content of the experimental samples.

Terminal void densities versus temperature and dose-rate are shown in Fig. 8 for a low dislocation density, expected to correspond to a solution-annealed sample. The open diamond symbols show observations taken from Ref. [19]. They correspond to experiments at 390 °C and 7.8×10^{-7} dpa/s, 411 °C and 3.1×10^{-7} dpa/s, or 430 °C and 0.91×10^{-7} dpa/s. The open triangles are from Ref. [20], open squares are from Ref. [21], plus sign + from Ref. [22], and crosses x from Ref. [23]. The filled circles represent measurements from Ref. [24]. Filled squares are taken from Ref. [25]; filled diamonds are from Ref. [26].

The highest number of voids develops at low temperatures, where the vacancy mobility is low so that many small clusters develop. Simultaneously, vacancy emission from these clusters is less frequent so that the critical cluster size is smaller. The predicted visible void density declines gradually with increasing temperature until a steep drop-off in void density occurs at high temperatures. This situation is shown most clearly in Fig. 9, where the dislocation density is higher and the displayed void densities span five orders of magnitude. The system has not finished nucleating voids at 100 dpa at the highest temperature limits of the curves in Fig. 9, so the densities there are not the true asymptotic values.

We may also examine trends in void number versus different, time-independent dislocation densities. The predicted terminal void densities typically increase with dislocation density. At higher temperatures, when void formation is prolonged, nucleation would occur

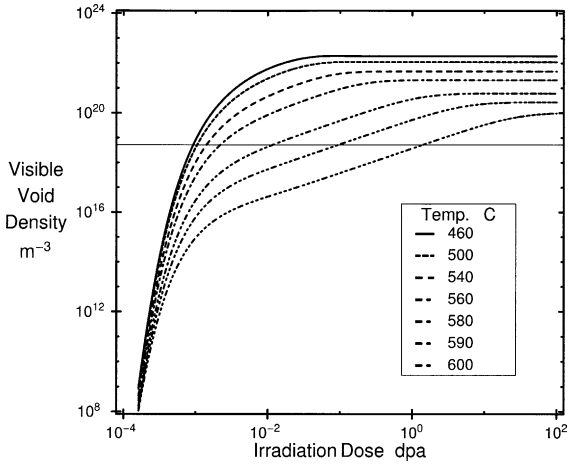

Fig. 7. 'Visible' void number density versus dose for a series of temperatures. Void densities below the thin horizontal line at 5×10^{18} m^{-3} are essentially undetectable by TEM. The irradiation rate is 10^{-6} dpa/s, and the dislocation density is held fixed at 6×10^{14} m^{-2}.

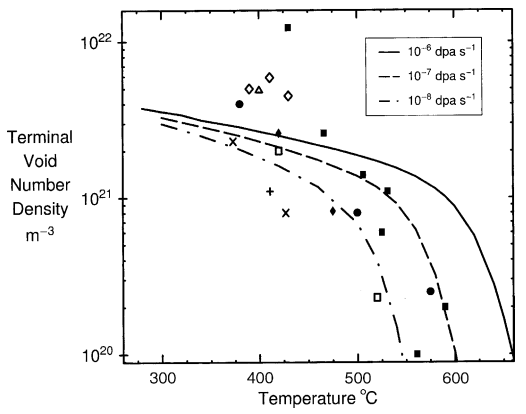

Fig. 8. Terminal visible void density is shown versus temperature for a fixed dislocation density of 2×10^{13} m^{-2}. The terminal density is achieved within a few dpa, at most. Experimental measurements are shown for comparison, open symbols are data for high-purity, ternary Fe–Cr–Ni alloys with 20% or less Ni from Refs. [19–23], and filled symbols are from Refs. [24–26], from earlier experiments on Ni and type-316 stainless steel.

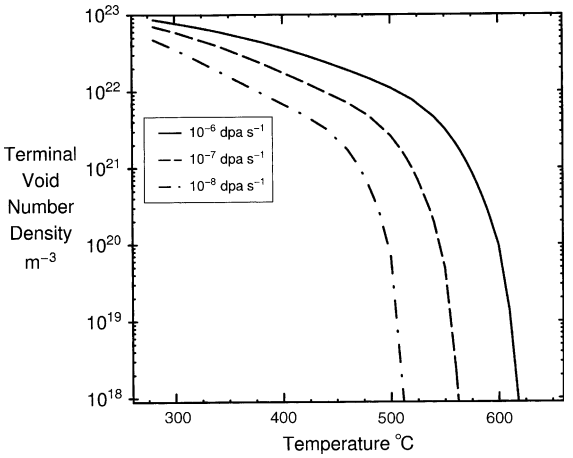

Fig. 9. Terminal (visible) void number density at 100 dpa versus temperature and dose-rate and for the constant dislocation density of 6×10^{14} m^{-2}.

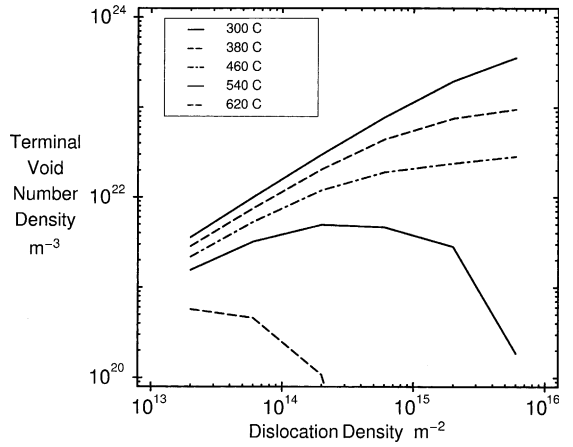

Fig. 10. Visible void density versus dislocation density after irradiation to 100 dpa at different temperatures.

concurrently with substantial changes in the dislocation content of the material, and the constant dislocation density calculations performed here will not be reliable. A complete theory thus requires the co-evolution of dislocation and void populations, especially for high temperatures (Fig. 10).

3. Conclusion

Recent systematic analyses of irradiation experiments reveal fundamental differences in the temperature and flux dependence of the incubation and steady-state periods. These newly-recognized characteristics contradict some of the traditional beliefs about radiation induced swelling. Since the controversy may affect projections for future nuclear reactor designs, it is worth performing a systematic comparison of theoretical models against the experimental data. Therefore, we have performed preliminary calculations for the nucleation and growth of voids in irradiated austenitic steel, to see if existing models are consistent with experiment. Our results are in general agreement with some observations of a dose-rate effect on the incubation period. The overall incubation behavior is qualitatively consistent with a 'temperature shift' versus irradiation dose-rate [18]. This shift plus the predicted shape of the incubation curve in Figs. 5 and 6, qualitatively explains the observed dose-rate effect on incubation. The qualitative agreement strengthens confidence in both the time-dependent nucleation and growth simulations and the recent experimental interpretations.

We employ a theoretical method that treats void nucleation and growth on the same footing. At this time, other components of the microstructure are not modeled as carefully. For example, there are no changes in dislocation density or microstructure, no dislocation loops, no impurity or solute migration or precipitate coarsening, and no introduction of helium in our simulations. These improvements will be added to successive generations of the model. Void nucleation proceeds despite the lack of gas impurities and in the absence of any production bias in the model. It occurs at all temperatures and dose-rates, although it can be very slow.

Consistent with the need for defect segregation to drive swelling, the nucleation of stable voids is typically complete before quasi-steady swelling is achieved. The remainder of the incubation delay is taken for the aggregate void sink strength to rise from its initial, negligible value. In general, we observe a very short incubation period, which is consistent with experiments in high-purity ternary stainless steel. All of our simulations should reach a maximum swelling rate (if run to sufficient times), after which the rate is slowly decreasing with time. The peak swelling rates from 450 to 650 °C lie between 0.7 and 0.9%/dpa, which is close to the experimental swelling rate of 1%/dpa for 316 SS. However, the swelling rates at late times are not universal; they vary with temperature and dislocation density. The difference may be due to our assumption of constant dislocation density. Swelling is sharply reduced at high temperatures because the incubation (void nucleation) times diverge. Changing the dose-rate seems mainly to shift the temperature-dependent incubation curve towards higher temperature. This shift, plus the shape of the incubation curve, appears to account for the so-called dose-rate effect.

The model currently deposits irradiation damage as mobile monomers, which vacancies then immediately begin to aggregate in voids. In actuality, damage is probably introduced as pre-formed clusters that must

evaporate and re-condense with voids or else migrate and coalesce with voids. Both processes will be incorporated in future models to see how they influence incubation and swelling behavior. The computational methods employed here will enable more thorough explorations of the various processes believed to influence void swelling, such as defect trapping by impurities, the concurrent evolution of dislocation loops and network dislocations, radiation-induced segregation and its impact on sink bias factors, 'production bias' and low-dimensional transport of defect clusters. Many of these are believed to influence the incubation dose, although their effects on the steady-state swelling may be smaller. It is useful to examine these processes individually in order to assess their relative importance and influence on one another. The study presented here, with fixed dislocation content, highlights the effects of void nucleation on the incubation and swelling behavior. It already reveals similarities with some experimental results. The effects of including a co-evolving aggregate dislocation density will be presented separately.

Acknowledgements

This work was performed under the auspices of the US Department of Energy by the University of California, Lawrence Livermore National Laboratory under Contract No. W-7405-Eng-48. This research was funded by the Department of Energy's Nuclear Energy Research Initiative (NERI) Program through the Office of Nuclear Energy, Science, and Technology.

References

[1] F.A. Garner, J. Nucl. Mater. 122&123 (1984) 459.
[2] F.A. Garner, J. Nucl. Mater. 205 (1993) 98.
[3] F.A. Garner, M.B. Toloczko, J. Nucl. Mater. 206 (1993) 230.
[4] F.A. Garner, M.B. Toloczko, B.H. Sencer, J. Nucl. Mater. 276 (2000) 123.
[5] F.A. Garner, in: B.R.T. Frost (Ed.), Materials Science and Technology: A Comprehensive Treatment, vol. 10A, Wiley, Weinheim, Germany, 1998, p. 410.
[6] T. Okita, T. Kamada, N. Sekimura, J. Nucl. Mater. 283–287 (2000) 220.
[7] T. Okita, T. Sato, N. Sekimura, F.A. Garner, in: Proceedings of the Fourth Pacific Rim International Conference on Advanced Materials and Processing (Aoba, Aramaki, Aobaku, Sendai, 2001), vol. PRICM-4.
[8] T. Okita, T. Sato, N. Sekimura, F.A. Garner, L.R. Greenwood, J. Nucl. Mater. 307–311 (2002) 322.
[9] T. Okita, T. Sato, N. Sekimura, F. A. Garner, L.R. Greenwood, W.G. Wolfer, in: Proceedings of the 10th International Symposium on Environmental Degradation of Materials in Nuclear Rower Systems – Water Reactors, 2001.
[10] R.E. Stoller, G.R. Odette, in: F.A. Garner, N.H. Packan, A.S. Kumar (Eds.), Radiation Induced Changes in Microstructure: 13th International Symposium (Part I), ASTM STP 995, vol. ASTM STP 995, ASTM International, West Conshohocken, PA, 1987, p. 371.
[11] A.D. Brailsford, R. Bullough, J. Nucl. Mater. 44 (1972) 121.
[12] M.F. Wehner, W.G. Wolfer, Philos. Mag. A 52 (1985) 189.
[13] W.G. Wolfer, B.B. Glasgow, Acta Metall. 33 (1985) 1997.
[14] M.P. Surh, J.B. Sturgeon, W.G. Wolfer, in: M.L. Grossbeck, T.R. Alien, R.G. Lott, A.S. Kumar (Eds.), Effects of Radiation on Materials: 21st International Symposium, ASTM STP 1447, vol. ASTM STP, ASTM International, West Conshohocken, PA, 2003, p. 1447.
[15] M.P. Surh, J.B. Sturgeon, W.G. Wolfer, J. Nucl. Mater. 325 (2004) 44.
[16] M.L. Jenkins, J. Nucl. Mater. 216 (1994) 124.
[17] L.K. Mansur, J. Nucl. Mater. 216 (1994) 97.
[18] L.K. Mansur, Nucl. Technol. 40 (1978) 5.
[19] T. Okita, Doctoral thesis, University of Tokyo, University of Tokyo, 2001.
[20] H. Kawanishi, S. Ishino, J. Nucl. Mater. 179–181 (1991) 534.
[21] N. Sekimura, S. Ishino, J. Nucl. Mater. 179–181 (1991) 542.
[22] T. Muroga, H. Watanabe, N. Yoshida, J. Nucl. Mater. 212–215 (1994) 482.
[23] H. Watanabe, T. Muroga, N. Yoshida, J. Nucl. Mater. 212–215 (1994) 503.
[24] J.L. Brimhall, B. Mastel, J. Nucl. Mater. 33 (1969) 186.
[25] P.J. Barton, B.L. Eyre, D.A. Stow, J. Nucl. Mater. 67 (1977) 181.
[26] H.R. Brager, J. Nucl. Mater. 57 (1975) 103.